Tube-wave reflection from a porous permeable layer with an idealized perforation

Andrey Bakulin, Shell International E & P, USA; Boris Gurevich, Curtin University of Technology, Australia; Radim Ciz, CSIRO Petroleum, Australia; Serge Ziatdinov, St. Petersburg State University, Russia*

Summary

Tube or Stoneley waves are known to interact strongly at low frequencies with poroelastic formations provided that flow is not restricted at the borehole-formation interface. Increased permeability leads to increased attenuation and decreased velocity of the tube wave. Such mechanism has been explored previously for characterizing fractures and permeable formations in open-hole acoustic logging. In this study we focus on the reflection response of low-frequency tube waves from various finite-size poroelastic structures. First, we examine a model of a thin reservoir and demonstrate good applicability of the approximate 1D effective wavenumber approach to describe the interaction of tube waves with porous formations. We confirm that higher permeability leads to higher reflection coefficient. Then we analyze a model of idealized (disk-shaped) perforations inside a poroelastic layer and show that it has higher reflectivity compared to washout zones of the same geometry but with no-flow conditions at the interface.

Introduction

Tube waves represent easily excitable and very abundant seismic signals that are often acknowledged as the biggest source of noise on borehole recordings. The interaction of higher-frequency tube waves (or Stoneley waves) with porous permeable formations during acoustic logging can be utilized to characterize fractures and permeable zones intersecting open boreholes (Winkler et al., 1989; Tang and Cheng, 1993; Kostek et al., 1998). In cased boreholes tube waves can be used for evaluating quality and parameters of hydraulic fractures (Medlin and Schmitt, 1994; Paige et el., 1995). To better understand these phenomena, White (1983) proposed an approximate 1D approach that provides simple analytic description of reflection and transmission of tube waves. Tezuka et al. (1997) demonstrated the validity of the 1D approach for modeling low-frequency tube waves in open boreholes surrounded by elastic formations. In this study we investigate how well the 1-D approach performs in the case of poroelastic layers and extend this approach to describe the reflection response of idealized disk-shaped perforations. Such a study is a first step towards quantitative interpretation of tube-wave responses for formation and fracture properties in cased perforated boreholes (Medlin and Schmitt, 1994; Paige et el., 1995).

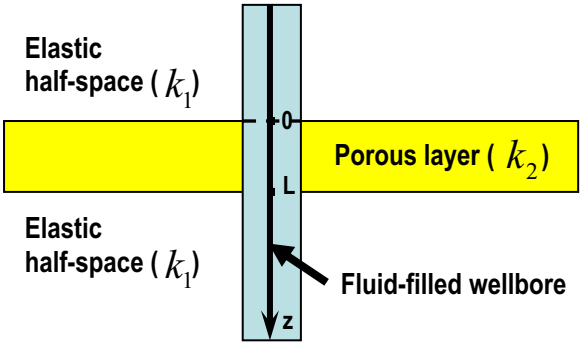

Figure 1: Model of fluid-filled borehole intersecting a porous zone in an elastic formation.

1D effective wavenumber approach

This study focuses on the theoretical analysis of the interaction of tube (Stoneley) waves, propagating along a fluid-filled borehole, with elastic and poroelastic layers embedded between two elastic formations (Figure 1). We adopt the 1D approach originally proposed by White (1983) and generalized by Tang and Cheng (1993). This formulation is quite general and no restrictions are placed on the nature of the borehole structures, except for radial symmetry. The theory is able to treat the tube-wave interaction with different borehole structures such as a elastic layers, permeable porous layers as well as diameter changes (washouts). In each homogeneous zone propagation is described by a 1D wave equation with constant effective wavenumber that depends on the properties of the surrounding formation as well as borehole parameters. To obtain the amplitudes of upgoing and downgoing waves, mass-balance boundary conditions are set at each interface, in particular, continuity of the fluid pressure and of the fluid displacement.

In the low-frequency regime, reflection and transmission coefficients from a single layer of any type are given by:

$$R = \frac{2i\left(k_2^2 - k_1^2\right)\sin(k_2 L)}{\left(k_1 + k_2\right)^2 e^{-ik_2 L} - \left(k_1 - k_2\right)^2 e^{ik_2 L}}, \qquad (1)$$

$$T = \frac{4k_2 k_1 e^{-ik_1 L}}{\left(k_1 + k_2\right)^2 e^{-ik_2 L} - \left(k_1 - k_2\right)^2 e^{ik_2 L}}, \qquad (2)$$

where L is the layer thickness, k_1 is the axial Stoneley wavenumber in the two half-spaces and k_2 is the axial Stoneley wavenumber in the layer. These expressions are

Tube-wave reflection from a porous layer with perforation

valid for a layer of any type as the rheology of the medium is absorbed by the effective wavenumber (Tang and Cheng, 1993). That is why we call this approach "effective wavenumber approach".

Stoneley wave propagation in the permeable zone is characterized by the effective wavenumber k_2:

$$k_2 = \sqrt{k_e^2 + \frac{2i\rho_f \omega \kappa(\omega)}{\Re \eta} \sqrt{\frac{-i\omega}{D}} \frac{K_1(\Re\sqrt{-i\omega/D})}{K_0(\Re\sqrt{-i\omega/D})}}, \qquad (3)$$

where K_1 and K_0 are modified Bessel functions of the second kind of the order one and zero, $\Re$ is the borehole radius, $\kappa(\omega)$ is the dynamic permeability, $D = \frac{\kappa(\omega)\rho_f c_f^2}{\phi\eta(1+\xi)}$ is the pore fluid diffusivity, ϕ is the porosity, ρ_f is the pore fluid density, c_f represents acoustic velocity of the pore fluid and ξ is a correction for the pore matrix compressibility (Chang et al., 1988). k_e is the wavenumber of the tube wave in an equivalent elastic formation given by

$$k_e = \frac{\omega}{c_T} = \omega\sqrt{\rho_f\left(\frac{1}{K_f} + \frac{1}{\mu}\right)}, \qquad (4)$$

with K_f being the fluid bulk modulus and μ formation shear rigidity.

At seismic frequencies the tube wavenumber (3) becomes complex-valued, exhibits strong dependence on formation permeability and behaves very differently from its elastic analogue (4) [Figure 2]. The deviation from the impermeable case is highest at lower frequencies and diminishes when frequency increases. Elevated attenuation and decreased tube-wave velocities are used as indicators for characterizing permeable zones in open-hole logging environment (Winkler et al., 1989).

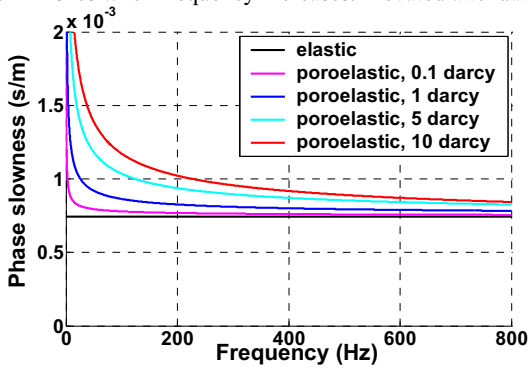

Figure 2: Phase slowness of tube wave $s = |k_2/\omega|$. The bottom straight line represents the slowness of an equivalent elastic layer. The other curves are for porous zones with varying permeability from 0.1 to 10 Darcy.

Model of a thin reservoir

Let us examine the accuracy of the effective wavenumber approach for the case of poroelastic formations. Such comparisons have been previously reported for irregular open boreholes surrounded by elastic formations (Tezuka et al., 1997) and fluid-filled fractures (Kostek et al., 1998). In both cases the effective wavenumber approach was shown to be in good agreement with direct computation of the wavefields by numerical methods. We are not aware of similar comparisons for poroelastic layers. Material parameters are listed in Table 1.

Parameters	*Formation*	*Fluid*	*Porous layer*
Bulk modulus K (GPa)	25.139	2.25	
Shear modulus μ (GPa)	16.875		
Density ρ (kg m^3)	2700	1000	
Grain bulk modulus K_g (GPa)			37
Grain shear modulus μ_g (GPa)			44
Grain density ρ_g (kg m^3)			3150
Dry bulk modulus K_0 (GPa)			11.452
Shear modulus μ (GPa)			9.3368
Porosity			0.35
Permeability (Darcy)			0-10
Viscosity (Pa s)		0.001	
Borehole radius (m)	0.142		0.142
Layer thickness (m)			2.4

Table 1: Model parameters used in computations.

Figure 3 (dashed lines) depicts tube-wave reflection coefficient as a function of frequency for the thin reservoir model from Table 1 computed with the effective wavenumber approach. Open boundary conditions are assumed between the borehole and the layer. Increase in layer permeability causes greater freedom for wellbore fluid to flow in and out of the poroelastic layer, leading to a larger reflection coefficient. Figure 3 also shows that a similar curves obtained with a finite-difference code jointly developed by Keldysh Institute of Applied Mathematics and Shell. Reflection coefficients were estimated by taking spectral ratios of incident and reflected tube waveforms. Good agreement between the two sets of curves is obtained above 80-100 Hz indicating that the effective wavenumber approach does capture the most important features of tube-wave interactions with poroelastic formations. Below 100 Hz the spectral-ratio calculations become less stable due to diminishing amplitudes in the input signal with 1000 Hz central frequency.

Tube-wave reflection from a porous layer with perforation

Idealized perforation model

Given success in describing tube-wave interaction for a single poroelastic layer using effective wavenumber approach, we decided to explore more complicated models with multiple layers. In particular, we focus on an "idealized perforation model" depicted in Figure 4. While the geometry and material parameters in this model are identical to those for the single-layer model of Figure 1, the key distinction is that two thirds of the interface between wellbore and the porous layer is now closed to flow.

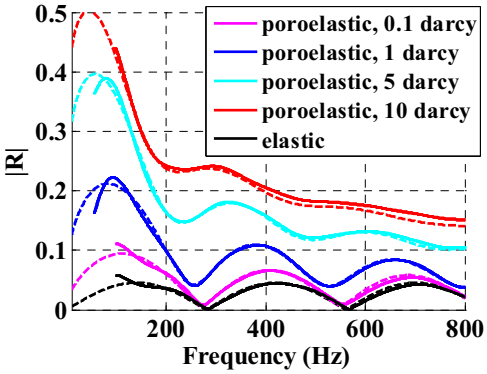

Figure 3. Amplitude of the tube-wave reflection coefficient as a function of frequency for a model with a single poroelastic layer (Figure 1 and Table 1). Dashed lines are derived with the 1D effective wavenumber approach, while solid lines are computed with a finite-difference code. The bottom curve represents reflection from the elastic zone between two elastic half-spaces.

Therefore fluid communication occurs only in the middle porous layer. Real perforation can be thought of as a small cylinder placed perpendicular to the borehole in a particular azimuth and thus it will have even more limited area of flow. For this reason we call our model "idealized (disk-shaped) perforation". Also, we do not account for the extra rigidity caused by the presence of steel casing in real boreholes, although in principle this should be possible. Even with these limitations the "idealized perforation model" is a useful first step since it can be treated by the cylindrically symmetric approaches at hand (effective wavenumber scheme and radially symmetric poroelastic finite-difference code).

First let us examine the interaction of the tube wave with a zero-length perforation ($w = 0$). From now on we fix the permeability of the porous zone to 1 Darcy. Due to the smaller area of fluid communication, the magnitude of the reflection coefficent decreases compared to the fully open case (Figure 1) and lies in between the curves for single poroelastic and single elastic layers (Figure 5). Recall that the elastic layer is equivalent to sealed (unperforated) poroelastic one. The multi-layered structure eliminates the sharp troughs that were present in the cases of single elastic or poroelastic layer. Overall we see good sensitivity of the

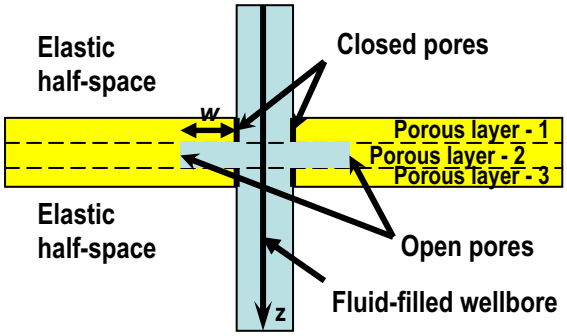

Figure 4: Idealized model of a disk-shaped perforation. All three porous layers have the same thickness (0.8 m) and identical material parameters from Table 1. Layers 1 and 3 have closed boundary conditions preventing flow from and into the borehole. Disk-shaped washout represents idealized perforation with length ***w*** and open boundary conditions at the ends.

reflection coefficient to the relative portion of wellbore-layer interface open to flow.

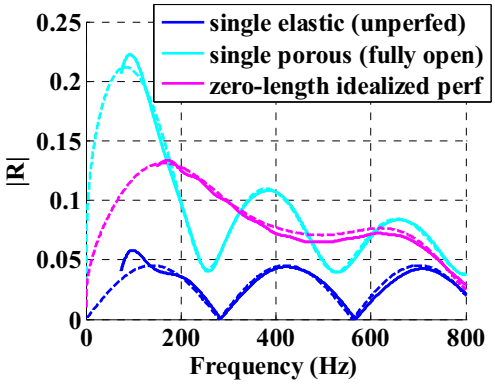

Figure 5: Reflection coefficient of tube waves from perforated and unperforated poroelastic layers. Permeability of porous zone is 1 Darcy. The dashed lines are derived with 1D effective wavenumber approach, while solid lines are computed with finite-difference code. The zero-length idealized perforation corresponds to the model of Figure 4 with $w = 0$. Elastic layer is equivalent to the unperforated poroelastic one and is shown for comparison.

An idealized perforation of a finite length causes a stronger reflection, since in addition to open flow we now have a change in the borehole diameter (Figure 6). If we close the

flow at the boundaries of the perforation, we end up with what is conventionally called a washout zone or enlargement in the borehole diameter examined in detail by Tezuka et al (1997). For this particular model the reflection coefficient from the washout zone is higher than that of zero-length perforation. Nevertheless, the reflection amplitude from the finite-length perforation is substantially larger than from the simple washout. Since the geometry of the models with washouts and finite-length perforations are identical, the difference between the reflection curves (cyan and blue in Figure 6) represents purely the effect of fluid flow into the porous layer via the open perforation.

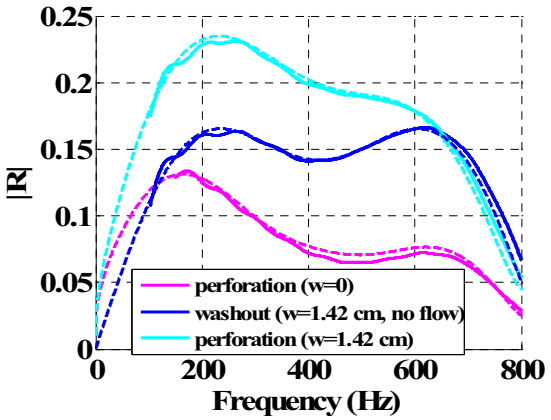

Figure 6: Reflection coefficient of tube waves from a layer with a single idealized perforation of various lengths. Permeability of porous zone is 1 Darcy. Dashed lines are derived with a 1D effective wavenumber approach, while solid lines are computed with a finite-difference code. Washout represents model identical to Figure 4 but with no-flow boundary conditions on the interface with the reservoir layer.

Conclusions

We have applied a 1D effective wavenumber approach to analyze interactions of low-frequency tube waves with stack of poroelastic and elastic layers. For the first time we have shown good agreement between responses obtained with 1D approach and finite difference computations.

We extended our analysis to cylindrically symmetric borehole irregularities inside poroelastic layers. In particular, we have examined the reflection response of a single idealized (disk-shaped) perforation inside the poroelastic layer. We have shown that cases of fully open-to-flow porous layer, fully sealed (unperforated) and partially sealed layer with finite-width and zero-length perforation can be distinguished for sufficiently large permeabilities of the formation. For finite-length perforations changes in borehole diameter further increase the reflection coefficent. Yet for the same geometry the washout (no-flow) and perforation (open flow) can still be distinguished by their low-frequency response. For the models at hand we observe larger reflection response for the perforation than for the washout. Realistic perforation geometries are 3D and therefore cannot be directly handled by 2D approaches. More theoretical and experimental work is needed to establish a proper 3D description of wave interactions with realistic cylinder-shaped perforations. Development of new analytical and computational approaches to tube-wave interaction with realistic 3D structures in cased boreholes may allow quantitative interpretation of the responses for properties of formation and hydrofractures. Perforation should be understood first since it is basic and abundant element present in majority of cased-hole completions.

References

Chang, S. K., Liu, H. L. and Johnson, D. L., 1988, Low-frequency tube waves in permeable rocks: Geophysics, 53, 519-527.

Kostek, S., Johnson, D. L., Winkler, K. W., and Hornby, B. E, 1998, The interaction of tube-waves with borehole fractures, Part II: Analytical models: Geophysics, 63, 809-815.

Medlin, W.L, Schmitt, D.P, 1994, Fracture diagnostics with tube-wave reflection logs: J. Pet. Tech., March, 239-248.

Paige, R.W., Murray, L.R., Roberts, J.D.M., 1995. Field applications of hydraulic impedance testing for fracture measurement: SPE Production and Facilities, Feb., 7-12.

Tang, X. M., and Cheng, C. H., 1993, Borehole Stoneley waves propagation across permeable structures: Geophysical Prospecting, 41, 165-187.

Tezuka, K., Cheng, C. H., and Tang, X. M., 1997, Modeling of low-frequency Stoneley-wave propagation in an irregular borehole: Geophysics, 62, 1047-1058.

White, J. E., 1983, Underground sound, Elsevier.

Winkler, K. W., Liu, H., and Johnson, D. L., 1989, Permeability and borehole Stoneley waves: Comparison between experiment and theory: Geophysics 54, 66–75.

Acknowledgements

The authors thank Shell International Exploration and Production for support and permission to publish this work.

EDITED REFERENCES

Note: This reference list is a copy-edited version of the reference list submitted by the author. Reference lists for the 2005 SEG Technical Program Expanded Abstracts have been copy edited so that references provided with the online metadata for each paper will achieve a high degree of linking to cited sources that appear on the Web.

Tube-wave reflection from a porous permeable layer with an idealized perforation
References

Chang, S. K., H. L. Liu, and D. L. Johnson, 1988, Low-frequency tube waves in permeable rocks: Geophysics, **53**, 519-527.

Kostek, S., D. L. Johnson, K. W. Winkler, and B. E. Hornby, 1998, The interaction of tube-waves with borehole fractures, Part II: Analytical models: Geophysics, **63**, 809-815.

Medlin, W. L., and D. P. Schmitt, 1994, Fracture diagnostics with tube-wave reflection logs: Journal of Petroleum Technology, **46**, 239-248.

Paige, R. W., L. R. Murray, and J. D. M. Roberts, 1995, Field applications of hydraulic impedance testing for fracture measurement: SPE Production and Facilities, February 7-12.

Tang, X. M., and C. H. Cheng, 1993, Borehole Stoneley waves propagation across permeable structures: Geophysical Prospecting, **41**, 165-187.

Tezuka, K., C. H. Cheng, and X. M. Tang, 1997, Modeling of low-frequency Stoneley-wave propagation in an irregular borehole: Geophysics, **62**, 1047-1058.

White, J. E., 1983, Underground sound: Elsevier.

Winkler, K. W., H. Liu, and D. L. Johnson, 1989, Permeability and borehole Stoneley waves: Comparison between experiment and theory: Geophysics, **54**, 66–75.